AuO: Evolving from Dis- to Comproportionation and Back Again

AuO: evolving from dis- to comproportionation, and back again

Andreas Hermann[*,1], Mariana Derzsi[*,2], Wojciech Grochala[2], and Roald Hoffmann[3]

[1] Centre for Science at Extreme Conditions and School of Physics and Astronomy, The University of Edinburgh, Peter Guthrie Tait Road, Edinburgh EH9 3FD, United Kingdom

[2] Centre for New Technologies, University of Warsaw, Żwirki i Wigury 93, 02089 Warsaw (Poland)

[3] Department of Chemistry and Chemical Biology, Cornell University, Ithaca, NY 14850, United States

Abstract

The structural, electronic, and dynamic properties of hypothetical gold(II)-oxide AuO are studied theoretically, at atmospheric and elevated pressures, with use of hybrid density functional theory. At p=1atm, hypothetical AuO (metastable with respect to the elements) is predicted to crystallize in a new structure type, unique amongst the late transition metal monoxides, with disproportionation of the gold ions to Au(I/III), and featuring aurophilic interactions. Under pressure, familiar structure types are stabilized: to a semiconducting AgO-type structure at ~2.5 GPa and, with further increase of pressure up to ~80 GPa, to an $AuSO_4$-type structure containing Au_2 pairs. Finally, above 105 GPa distorted NaCl-type and CsCl-type Au(II)O structures dominate, and metallization is predicted at 329 GPa.

1. INTRODUCTION

When Tutankhamen's tomb was opened, the gold objects in it gleamed as on the day the tomb was sealed. Of course, the reason for this is in the electrochemical series – almost anything in the world will reduce gold ions to metallic gold. Oxides of gold thus do not appear likely candidates for stability; nevertheless Au_2O_3, with a positive heat of formation, exist, and has been studied theoretically together with Au_2O.[1] In this and a subsequent paper we examine the potential of AuO.

1:1 AuO is not yet known; perhaps that is a good enough reason to study it. There is another motivation for looking at AuO, deriving from the peculiarities of the group 11 oxides above Au.[2] AgO is a "frozen" mixed valence compound with disproportionated Ag(I) and Ag(III) ions, linearly and square-planar coordinated, respectively. In CuO, copper, which usually takes on oxidation states +2 and +1, is clearly Cu(II).[3] In the high-T_c cuprates that oxidation state can be tuned by substitution, up and down from +2. And there is a hint that the oxidation state fluctuations Cu(I) ↔ Cu(II) ↔ Cu(III) play a role in the high T_c in these compounds.[4,5]

The question is then not only that of the potential existence (perhaps under pressure) of AuO, but also what will the Au ions do in such a compound – will they be in oxidation state +2, or will they disproportionate to +1 and +3, as one finds in AgO? And what will be its conducting properties? Pressure is another variable that has been used to tune the transition to superconductivity in the cuprates,[6] and so it will be instructive to play with this variable in AuO.

2. COMPUTATIONAL METHODOLOGY

The VASP package was used to perform density functional theory calculations, using the PBE, the PBEsol, and the hybrid HSE06 exchange-correlation functionals, and different 'projector augmented wave' (PAW) 'frozen core' choices with corresponding plane wave basis sets.[7–12] To uncover enthalpically relevant structures for AuO, we performed evolutionary structure searches with the XtalOpt package.[13] The structure search approach, which

complements chemical or physical intuition, has been used successfully, particularly to study high-pressure phases of compounds.[14–18] Here, structure searches with four formula units per cell were performed at pressures of 1 atm, 100 GPa, 200 GPa, 300 GPa, and 400 GPa, using the PBE functional with "soft" PAW data sets and a plane wave cutoff of 300 eV. Additional pressure points were scrutinized only for selected structures, those that were relevant to phase transitions occurring in given pressure regions. Structural candidates were then re-optimized across the entire pressure range with the PBEsol functional and "hard" PAW data sets (including 6 and 17 valence electrons for oxygen and gold, respectively), and a corresponding plane wave cutoff of 800 eV. The PBEsol functional is a re-parameterization of the PBE functional suitable for solids, and generally gives better agreement with experiment regarding lattice constants, elastic properties, and (for compounds with ionic bonding components) cohesive energies.[19,20]

Structures were optimized until remaining forces were below 1 meV/Å. Brillouin zone integrations were performed on regular k-point grids with a linear spacing of 0.16 $Å^{-1}$. Electronic band structures and density-of-state (DOS) calculations were carried out with both the PBEsol and the hybrid HSE06 functional, using geometries optimized at the respective level of theory. Crystal structure optimizations using the CPU-demanding hybrid HSE06 functional were done with a plane wave cutoff of 500 eV, and k-spacing of 0.35 $Å^{-1}$. Additionally, enthalpies and electronic densities of states were recalculated with denser k-spacing of 0.24 $Å^{-1}$ for structures optimized with the hybrid HSE06 functional. The pressures of the phase transitions at the HSE06 level were obtained using linear interpolation between adjacent computed pressure values.

Normal modes at the zone center were calculated for the most important structures using VASP.[7,8] Vibrational ZPE was found to have negligible effect on stability, and was not considered. Every structure examined in this paper is a ground state static phase, i.e., there is no consideration of the temperature-mediated influence of entropy on structural stability.

3. RESULTS AND DISCUSSION

AuO at atmospheric pressure Our structure searches at P=1 atm resulted in a variety of candidate structures, see Figure 1. Amongst those are known metal oxide structure types (more on those below), and others that are new. In particular, we find AuO to be most stable in a monoclinic *C2/c* structure, a new structure type not seen in other transition metal oxides. The structure does, however, recite features of the CuO, mixed valence AgO ($Ag^{1+}Ag^{3+}O_2$), and PdO structures. The difference between these and the AuO structure is perhaps not too surprising, given the so-called "aurophilic interactions" between the metal atoms of the latter;[21–23] more of this anon.

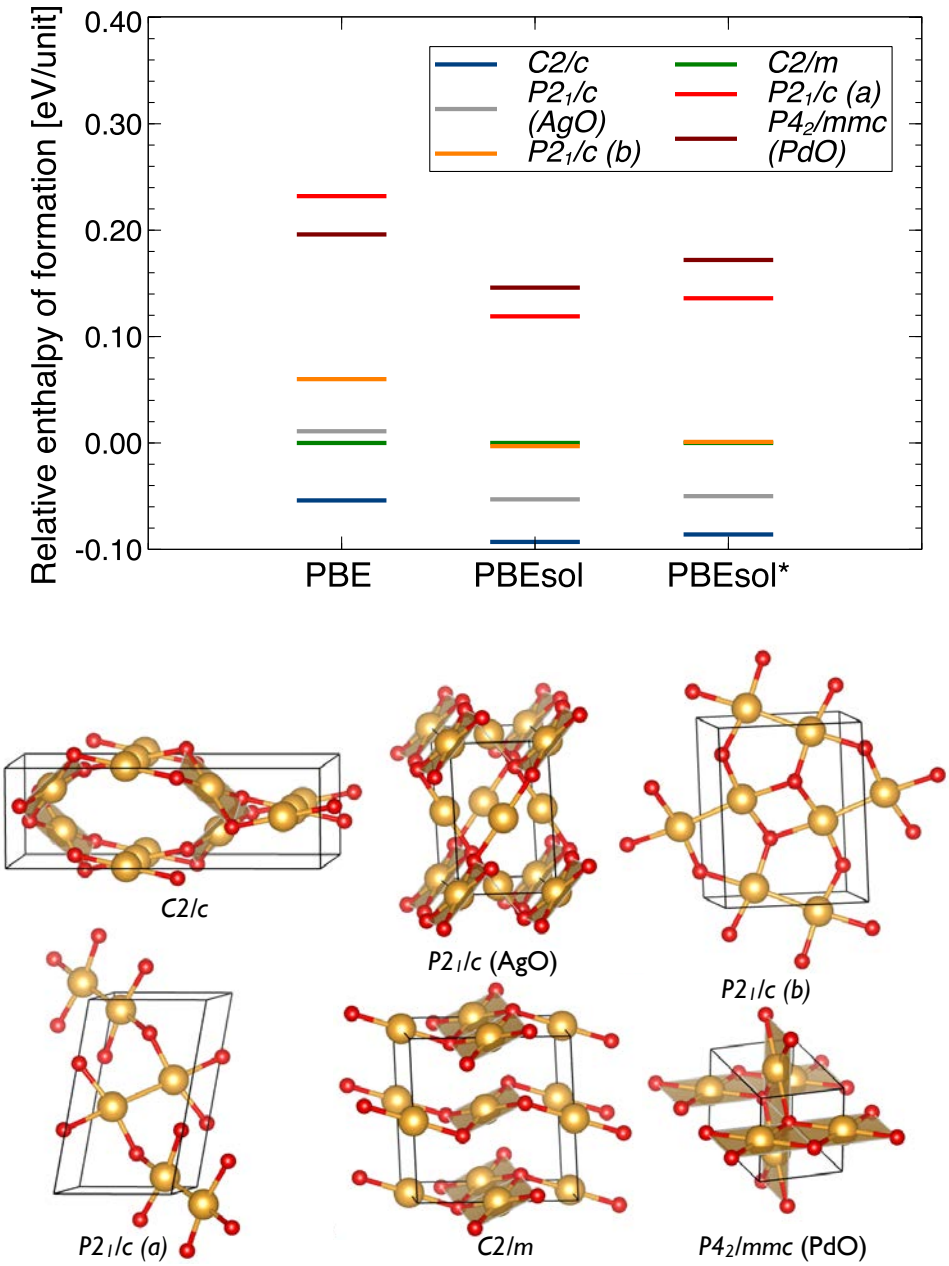

Figure 1. Enthalpies of formation (top, relative to the C2/m structure) and structures (bottom) of selected low-energy AuO phases at atmospheric pressure as obtained from crystal structure prediction; functionals used are indicated, PBEsol* refers to using "hard" small-core PAW data sets. Gold (oxygen) atoms are shown as golden (red) spheres, structures are from PBEsol* optimizations.

CuO crystallizes in a monoclinic structure, space group *C2/c*, where all copper atoms are identical, and connected in a nearly planar geometry to four oxygen atoms, see Figure 2.[24,25] Though sharing a common space group with our best AuO structure, the CuO geometry differs in detail. In it, each oxygen atom is in turn shared between four copper atoms. Overall, the structure has doubly-bridged chains of copper atoms running through the lattice, which alternate direction along the *c* axis, and are not quite orthogonal to each other. The copper

atoms, being Cu(II), have a d^9 electronic configuration, which explains their departure from octahedral coordination (in a parent NaCl structure[26]) toward a square-planar one. Cu(II) complexes sometimes also show a distortion from square planar toward tetrahedral coordination, as in $CuCl_4^{2-}$.[27,28] The CuO structure is a distorted variant of the tetragonal PdO structure (space group $P4_2/mmc$), where each Pd atom is ideally square-rectangular coordinated, and the bridged chains of Pd atoms are orthogonal within the *ab* plane.[29,30] In Figure 2, this relationship between CuO and PdO, but also with AgO and the proposed AuO structure, is shown.

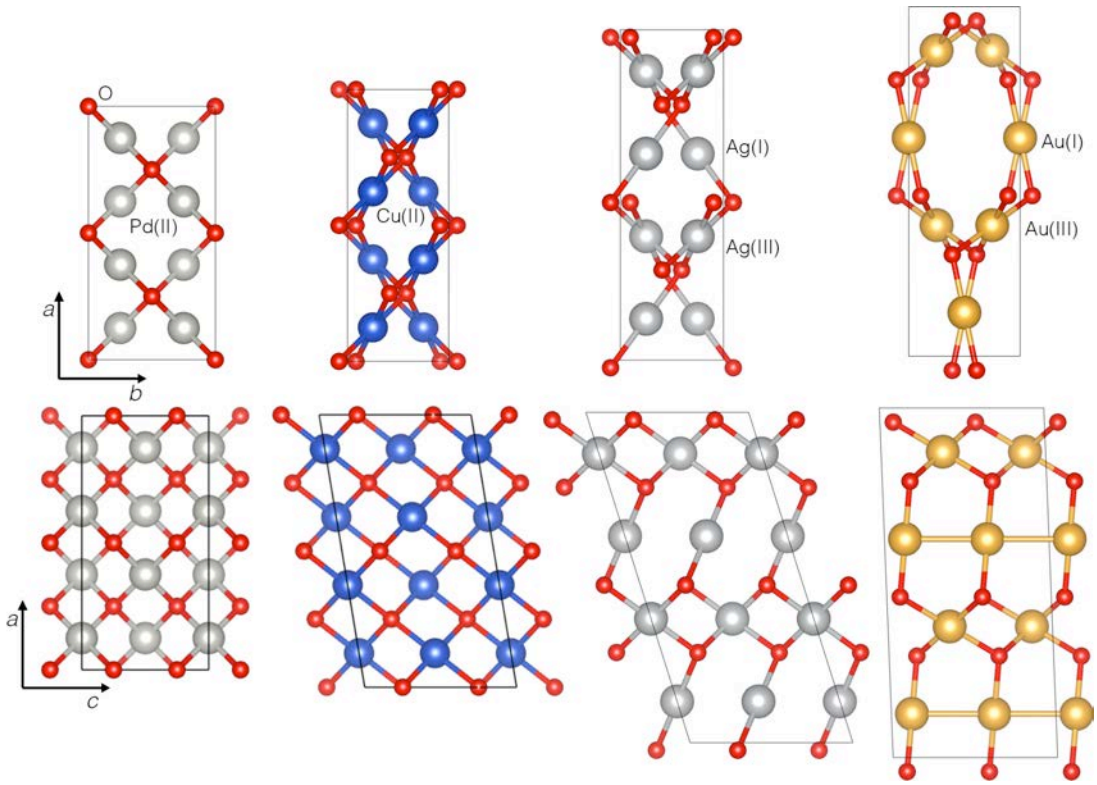

Figure 2. Crystal structures of some of the late transition metal oxides at atmospheric pressure, as seen along the *c* axis (top) and *b* axis (bottom). From left: PdO, $P4_2/mmc$ structure; CuO, $C2/c$ structure; AgO, $P2_1/c$ structure; proposed AuO $C2/c$ structure. In AuO, proposed aurophilic Au(I)-Au(I) interactions are drawn as gold lines. All structures are drawn to the same scale, and were optimized with the PBEsol functional.

One of the known AgO polymorphs also crystallizes in a monoclinic structure (the other being tetragonal), space group $P2_1/c$. But it prefers a clearly disproportionated structure, with linear coordinated Ag(I) atoms (electronic configuration d^{10}) as well as square-planar Ag(III) atoms (electronic configuration d^8).[31] The actual structural difference between CuO and $P2_1/c$-AgO is relatively small and both deviate little from the PdO structure,[32] see Figure 2.

In fact, both phases can be seen, together with PdO and other late transition metal oxides, as deformations of the rock salt structure; the differences between them may be explained in terms of coordination chemistry and collective Jahn-Teller effects.[26,33]

For AuO, all the structures mentioned above were found as local minima during the evolutionary structure search, with the AgO structure being the most stable of these. This energetic order is not surprising, as one might have expected a disproportionated structure for AuO. The global minimum ($C2/c$), however, is 36 meV per formula unit more stable than the AgO structure, and is shown in both Figure 1 and Figure 2 (see the SI for crystallographic information on this and all other relevant AuO phases discussed throughout). Through a slightly different coordination network (compared to AgO), linear –Au-Au-Au– chains form within the structure (see Figure 2). Along those chains, Au(I)-Au(I) separations are 2.78 Å. This separation is short, and much shorter than the Au(III)-Au(III) separations (3.36 Å) in the same structure, as well as Ag(I)-Ag(I) and Ag(III)-Ag(III) (both 3.26 Å) in AgO. Linear chains of Au atoms have been found in the crystal structure of inorganic Au polymeric complexes, albeit with longer Au-Au distances of 2.91-3.11 Å.[34] Just like in PdO, CuO, and AgO, this structure for AuO can be traced back to a distorted rocksalt structure – though with larger distortions than for the other compounds. In analogy to our earlier work,[26] the corresponding matrix transformation relative to the rock salt archetype, and atomic displacements from it are given in the SI.

We thus identify the interaction between the Au(I) ions as an aurophilic interaction. Originally traced to d_z^2-s,p mixing,[35–38] this closed shell-closed shell, d^{10}-d^{10} interaction has been reassigned to exchange interactions beyond the Hartree-Fock level, essentially a strong correlation-dispersion interaction with a significant relativistic contribution.[39–41] The nominal oxidation state of the Au ions can be corroborated with partial charges from a Bader analysis of the total charge density, which are +0.47 for Au(I) and +1.12 for Au(III) and, consequently, -0.79 for the O ions (all numbers from the PBEsol functional). We are well aware that formal oxidation states are a convenient fiction, and the relationship of

calculated charges -- by whatever uniquely defined but arbitrary method one uses to calculate them – to oxidation states is muted.

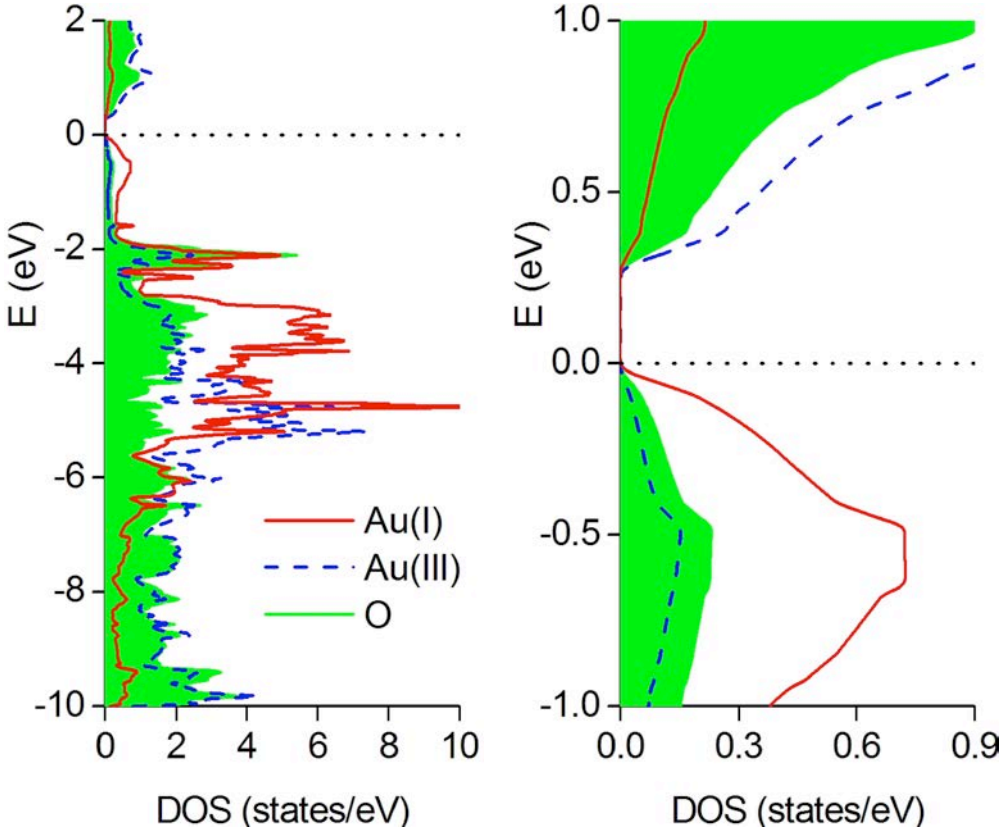

Figure 3. Atomic projections of electronic DOS of *C2/c*-AuO at ambient pressure (from HSE06). Left: the -10 to +2 eV energy range; right: focus around the band gap region.

The mixed valence character of AuO is further evident from the electronic density of states (DOS, see Figure 3). The electronic structure is dominated by Au(5d) states, with O(2p) states mixing in. However, the partial DOS for Au(I) is substantially different from that of Au(III) in the broad energy window. One significant difference is that Au(III) states are on average at larger binding energies that those of Au(I). This should be expected based on both formal oxidation states as well as Bader charges.

It will be noted that the Au(I) states make up most of the top of the valence band while the Au(III) states predominate in the conduction band. This, too, is anticipated for a classic mixed-valence system, for which the inter-valence charge-transfer excitations should contribute most to the electronic conductivity. For AuO, the valence band is composed mostly of the lone pairs at the Au(I)

cation (a combination of 5d(x^2–y^2), 5d(z^2) and relativistically stabilized 6s orbitals) while the conduction band is made of empty Au-O antibonding 5d(x^2–y^2)/6s states of Au(III). AuO, i.e. Au(I)Au(III)O_2, should thus be not much different in this respect from AgO – a prototypical d^{10}/d^8 frozen valence system.[42]

The aurophilic interactions directly influence the electronic properties of AuO in the GGA description, rendering this system metallic at P = 1 atm (cf. SI). Using the hybrid HSE06 functional that includes screened exchange interaction, AuO has a small band gap of 0.27 eV (see Figure 3). This band gap is much smaller than those of Si (1.11 eV), Ge (0.67 eV), PbS (0.41 eV) and comparable with that of PbTe (0.31 eV). If prepared -- more on its stability below -- AuO would thus be a very narrow band gap semiconductor. The closest (in enthalpy) metastable structural alternative to the *C2/c* structure, the *P2₁/c* AgO-type structure, lacks the aurophilic interactions and has (at the HSE06 level of theory) a band gap of about 0.98 eV (or 0.2 eV at PBEsol level of theory). The calculated band gap of AuO in the *P2₁/c* AgO-type structure is very similar to that computed recently for related AgO in the same structure type (0.94 eV[43]).

In our calculations, we find AuO to be stable with respect to decomposition into Au+1/2*O_2 by 89meV/unit at HSE06 level of theory, or 59meV/unit at PBEsol level of theory. Note that DFT functionals, hybrid or otherwise, have problems describing the magnetic ground state of solid oxygen, [44,45] and these formation enthalpies are thus less certain than one would like. A synthesizable system in the solid state should also exhibit dynamic stability, i.e. all its phonon frequencies must be real. We have calculated phonon modes at the zone center with both PBEsol and HSE06. All phonon modes are real (*cf.* SI), attesting to the dynamic stability of the *C*2/c polymorph.

AuO under pressure: first, an AgO structure The ground state structure of AuO at P=1atm is overall rather open, having quite wide "channels" along the *c* axis (clearly seen in Figure 2). This leads to a volume per formula unit of ~31.1 Å^3 -- which agrees with an estimated volume of 30.3-33.1 Å^3, as calculated from the difference of the corresponding volumes of $AuSO_4$ (88.25 Å^3)[46] and SO_3

(55.12-57.96 Å^3).[47,48] When external pressure is applied, phase transitions to more compact, close-packed structures should be expected. Indeed, this is the case. We find with the HSE06 functional that at a mere p=0.8 GPa (2.5 GPa with PBEsol) the *P2$_1$/c* AgO-type structure becomes more stable, see Figure 4. This structure, discussed above, also contains Au(I) and Au(III) ions, but the directions of the linear O-Au(I)-O units allow for more compact packing: at the transition pressure, the unit cell of the *P2$_1$/c*-AgO structure is 9 vol-% smaller than that of the *C2/c* structure (7 vol-% with PBEsol).

Note that increase in pressure also leads to a rapid stabilization of the decomposition product, indicated as dashed line in Figure 4. Eventually, at very high pressures exceeding 370 GPa, we find AuO becoming stable again compared to the elements .

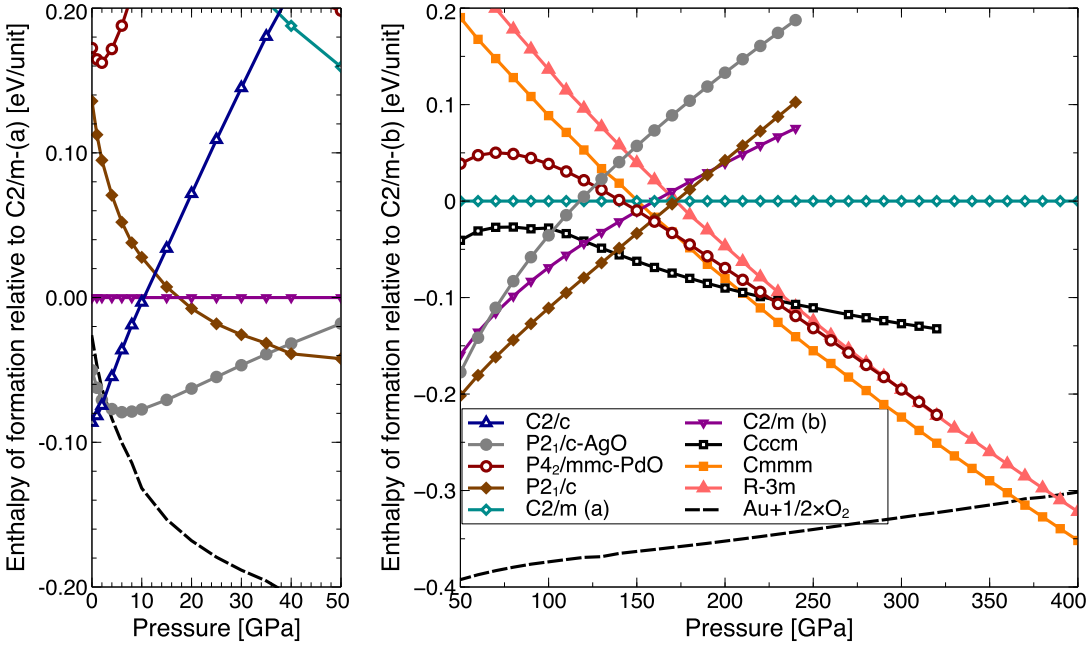

Figure 4. Relative enthalpies of formation for AuO structures as a function of pressure, from PBEsol calculations. Left plot shows the low-pressure regime below 50 GPa, right plot the high-pressure regime above 50 GPa. Note different enthalpy scales and different baseline structures. The enthalpy of the elements, Au+1/2*O$_2$, is shown as the dashed line. See the SI for the volume changes with pressure for the most relevant structures.

Higher pressure: comproportionation in the AuSO$_4$ structure At p=82 GPa (37 GPa with PBEsol) another *P2$_1$/c* structure becomes the most stable phase of AuO. The structure (see Figure 5) is distinguished in two ways: firstly, this is the pressure of comproportionation, where all gold atoms attain identical

coordination environments, and are thus formally in the Au(II) oxidation state. A Bader charge analysis[49] with the PBEsol functional assigns at p=80 GPa a partial charge of +0.84e to the Au(II) ion, very close to the mean of the Au(I)/Au(III) charges (+0.85e, see above). Secondly, it features Au-Au dimer units bound by what appears to be a two-electron chemical bond and not just an aurophilic interaction: the Au(II) atoms are square-planar coordinated, leaving one electron pair for the Au-Au bond; the separation (2.42Å at 80GPa) is much shorter than a typical aurophilic separation (or 2.67Å in fcc-Au metal); and the bond is significantly less compressible (it is 2.66Å at 1atm) than an aurophilic interaction. Distinct Au_2O_6 units can then be perceived in this structure, with all O atoms shared between adjacent units. Salts of M_2L_6 with direct M-M bonds, where M is a group 10 metal, have been characterized; in those, the square-planar coordinated ML_3 units are usually perpendicular to each other,[50–53] unless bridging groups enforce an overall planar geometry.[54–57]

In our recent work, we emphasized structural similarities between late transition metal oxides and their respective sulfates – with the O^{2-}- and $(SO_4)^{2-}$-sub-lattices being close to each other.[26] A plausible structure for AuO could then be gained from known $AuSO_4$ by substitution $SO_4 \rightarrow O$. The *$P2_1/c$* structure discussed here is identical to the most stable AuO structure obtained from such a substitutional *ansatz.*[58] The relation between oxide and sulfate found in other late transition metals thus carries over to the case of gold as well, but restricted to a certain range of elevated pressure.

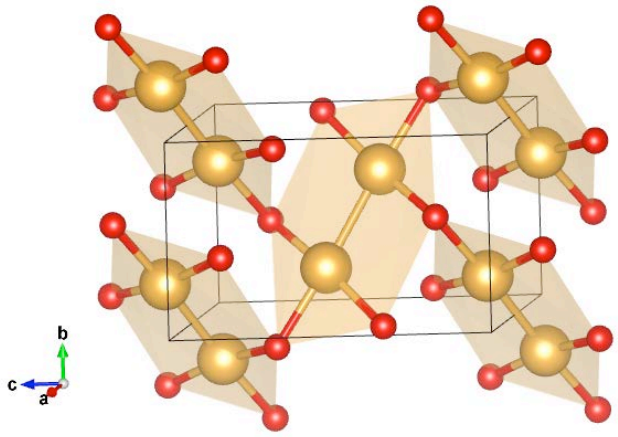

Figure 5. The high-pressure *$P2_1/c$* phase of AuO, shown here at p=82 GPa (from PBEsol functional). Au_2O_6 units are emphasized.

Still higher pressures: relatives to the NaCl and CsCl structures At even higher pressure, around p=105 GPa (137 GPa with PBEsol), more close-packed structures are stabilized, and the Au_2 dimer feature becomes unfavorable. The most stable structure between 105 GPa and 329 GPa is orthorhombic, of *Cccm* symmetry, and features square-planar coordinated Au(III) ions alternating with square nets of non-classical cubic coordinated Au(I) ions, see Figure 6. We see here the appearance of the ionic CsCl B2 structure: the square-planar coordinated Au(III) ions, together with the O atoms, form a severely distorted B2 sub-lattice (so we have effectively 4 + 4 coordination); whereas the square-net Au(I) ions, together with the O atoms, form an almost perfect B2 sub-lattice. The coordination polyhedra of the two different Au sites, shown in Figure 6, illustrate these two different environments. This structural interpretation is corroborated by a Bader partial charge analysis: at p=200 GPa, the Au(I)/(III) sites have a partial charge of +1.03/+0.69e, with a corresponding partial oxygen charge of -0.86e. Thus, AuO is again disproportionated in this pressure range.

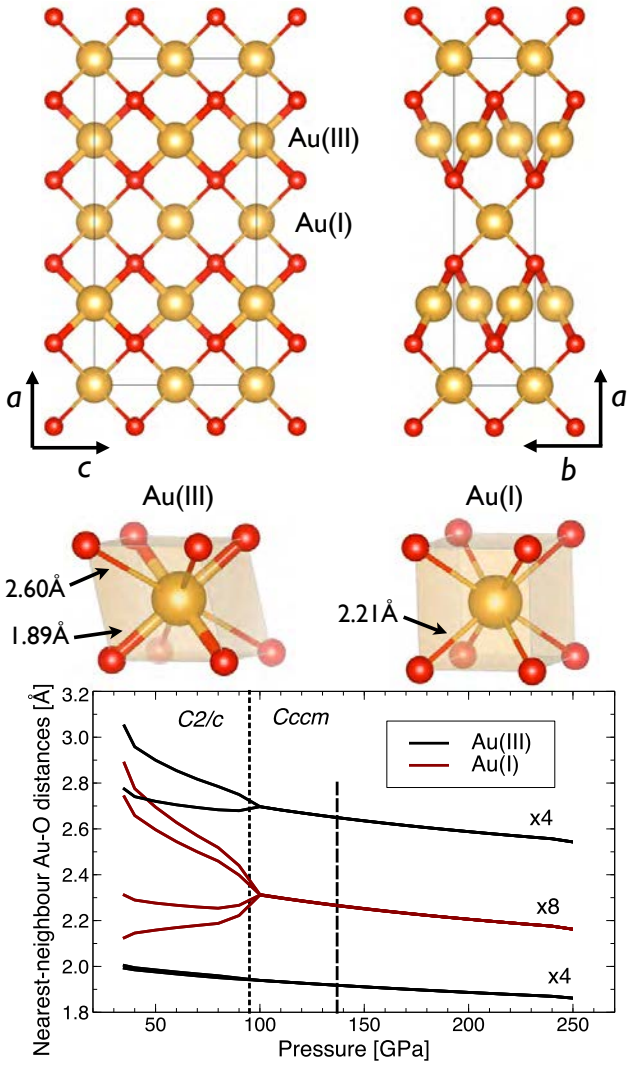

Figure 6. Structural features of *Cccm*-AuO at p=200 GPa, optimized with the PBEsol functional. From top to bottom: two views of the structure, with different Au sites labeled; the coordination polyhedra of the Au sites, with nearest neighbour Au-O distances indicated; and the evolution of those Au-O distances (with four- or eight-fold degeneracy pointed out) as function of pressure. Below 95 GPa, the *Cccm* structure optimizes with PBEsol to a lower-symmetry metastable *C2/c* structure; above 137 GPa, the *Cccm* structure is stable.

At pressures above p=329 GPa (210 GPa with PBEsol), comproportionated close-packed orthorhombic and rhombohedral structures are most stable. Enthalpies of formation of the latter are shown in Figure 4, and the respective structures themselves in Figure 7. The lowest-enthalpy *Cmmm* structure is an orthorhombic compression (for its primitive cell at p=330 GPa: a/c = b/c = 0.955) of the B2 (CsCl) structure, and the *R-3m* structure is on the rhombohedral structural transition (Buerger[59]) path connecting the B1 and B2 structures (at p=330 GPa: α=83.1°, where α=90° corresponds to the B2, and α=60° to the B1 structure), see Figure 8. Moreover, the *Cmmm* structure is an intermediate along the more sophisticated B1-B2 transition paths suggested by

Watanabe *et al.*[60] and Tolédano *et al.*,[61] and also the global minimum along both those paths (see the SI for the corresponding potential energy surfaces). At p=365 GPa (with PBEsol), the *Cmmm* structure becomes stable against decomposition into the elements, see Figure 4. With the HSE06 functional, this stabilization is found at slightly lower pressures, just above 300 GPa, and still in the stability region of the *Cccm* structure.

The *R-3m* and *Cmmm* structures are connected through a monoclinic distortion, as shown in Figure 8. The monoclinic distortion of the *Cmmm* structure, which involves sliding of adjacent Au layers along the *c* axis, results in a set of monoclinic *C2/m* structures. This distortion eventually results in the rhombohedral *R-3m* structure with γ=β=α=83.1° (at p=330 GPa). The latter (where every Au atom has "6+2" coordination in O) is less favorable than the *Cmmm* structure, where the Au-O coordination is "4+4", thus allowing a close packing while keeping square-planar Au coordination intact. But the *R-3m* structure is a local minimum along the transition path from the NaCl-B1 to the CsCl-B2 structure (where the Au-O coordination is 6 and 8, respectively).

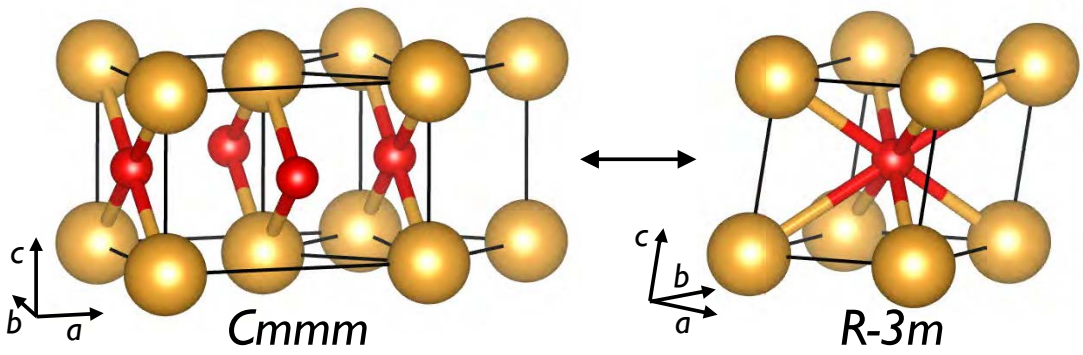

Figure 7. High-pressure *Cmmm* and *R-3m* phases of AuO shown at 330 GPa. The primitive unit cell of *Cmmm* (with Z=1) is also indicated.

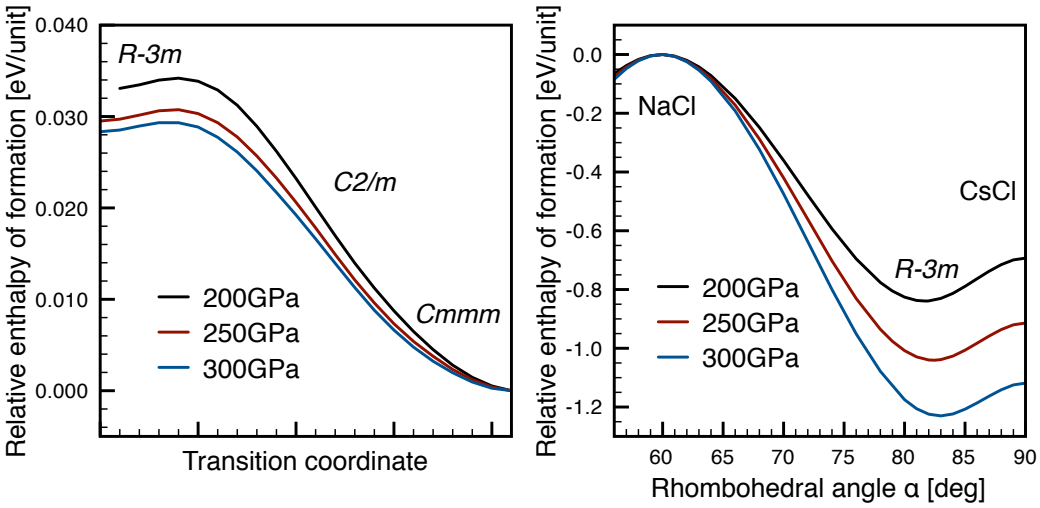

Figure 8. Left: continuous transition between the lowest-enthalpy high-pressure structures, *R-3m* and *Cmmm*. Right: continuous transition between the NaCl-B1 and CsCl-B2 structures along the Buerger path, with the *R-3m* structure as local minimum. All enthalpies obtained from PBEsol calculations.

It is remarkable that even at pressure as large as 350 GPa, the d^9 cation -- Au(II) here -- preserves its preference for the square-planar geometry. This may be viewed as a manifestation of pronounced steric activity of the 5d(z^2) lone pair, which is well known for both Au(III)[62] and Au(II) compounds[63] at 1 atm.

It seems that there is use for chemical intuition, here preferences in coordination environment as function of electron count, applied to matter compressed to 3.5 mln atm.

Evolution of band gap at the Fermi level of AuO with external pressure The evolution of the fundamental electronic band gap of AuO as function of pressure is of interest. We have studied the electronic structure of various crystalline forms of AuO up to 400 GPa (see Figure 9 and Figure 10, and the SI for DOS calculated at PBEsol level of theory).

As already mentioned, the *C*2/c polymorph, which is the lowest energy structure at 1 atm, has a small band gap of 0.27 eV calculated with the hybrid HSE06 functional (but artificially closed in the PBEsol calculations). It might be expected that such a small band gap could be closed rather easily with pressure, and indeed, the gap is computed to be null at pressures below 20 GPa. However, as already discussed, a phase transition at 0.8 GPa should take place to the $P2_1$/c-

AgO structure type. This new polymorph has a band gap of ~1.0 eV at the phase transition, and its gap is not as easily closed as that of its predecessor -- it maintains a band gap throughout its region of stability, see Figure 9. A similar mechanism for preserving a quasi-gap in compressed AgO[43] brings to mind Pearson's Maximum Hardness Principle.[64]

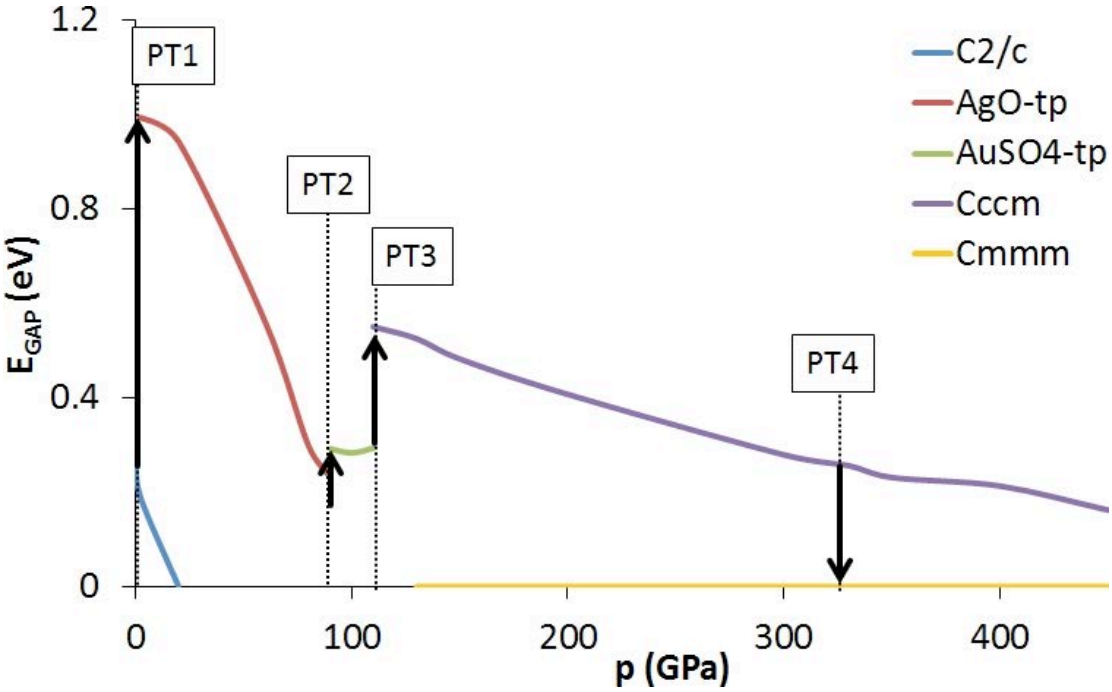

Figure 9. The progression of the fundamental electronic band gap for various polymorphic forms of AuO. The stability limits of various polymorphs have been marked, where "PT" denotes the various phase transitions. All calculations here are with the HSE06 functional. Note that the PBEsol functional predicts all these structures to be metallic across the entire pressure range.

The next phase transition related to comproportionation (to the $AuSO_4$-type structure) is computed to take place at 82 GPa. At this pressure, the band gap for the *P2₁*/c-AgO structure is ~0.20 eV, while the value for the resulting $AuSO_4$ polytype is very similar, ~0.28 eV. Interestingly, the band gap of this polymorph tends to be quite constant up to 100 GPa, and then even begins to slightly increase with pressure rather than decrease (Figure 9). The next phase transition, connected with subsequent disproportionation, has been predicted to occur at 105 GPa. The resulting *Cccm* polytype turns out to have much larger band gap than its predecessor, over 0.5 eV at the phase transition. We see the Maximum Hardness Principle at work again, and despite a considerable compression. This new structure, too, maintains a finite (hybrid-DFT) band gap throughout its stability range and even beyond 450 GPa (!).

At 329 GPa the pV term related to packing of the crystal structure, which is a key factor influencing stability at high pressure, drives the transition from the *Cccm* to to the *Cmmm* phase. The *Cccm* polytype at this pressure has a bandgap of 0.26 eV, comparable to that of the ambient-pressure *C*2/c form (!). This example is instructive for realizing of how stubbornly AuO resists metallization to 329 GPa. At this pressure the band gap finally closes for the thermodynamically preferred *Cmmm* type – which is the first unambiguously metallic AuO phase. It is only at this immense pressure that the electronic arguments related to Pearson's hardness no longer apply and close(st) packing has its say.

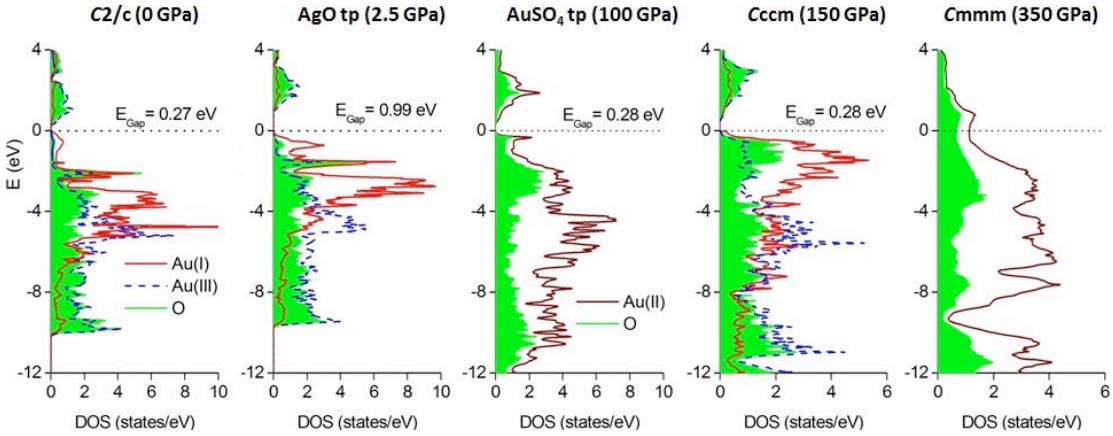

Figure 10. The partial DOS (HSE06) for various polymorphic forms of AuO at pressures selected from the regions of their thermodynamic stability.

The electronic DOS for the *Cmmm* structure at 350 GPa (Figure 10) shows the expected splitting of the Au *5d* bands, with (in this case of square-planar coordination) a significant stabilization of the in-plane d_{xz} and d_{yz} orbitals. Still, significant band overlap makes this phase a relatively good metal, at both levels of theory considered (HSE06 and PBEsol). Interestingly, this polytype is structurally two-dimensional, with an appreciable difference between intra-sheet and inter-sheet Au–O separations of ~15% (at 330 GPa); this renders the *Cmmm* structure a 2D metal, as evident also from inspection of its band structure (*cf.* Figure SI 5 in SI). The comproportionated *Cmmm* structure realizes a genuine Au(II)O formulation and should be the lowest-enthalpy polymorph of AuO up to 400 eV, where our scrutiny ends.

AuO should resist metallization up to pressures beyond the metallization pressure of O_2 alone (> 100 GPa).[65] It should be stressed here that the semilocal PBEsol functional is incapable of predicting the finite band gap for all polymorphic forms of AuO except the *Cmmm* one. This well-known deficiency of standard DFT methods should discourage researchers from applying it to predictions of the electronic structure of novel compounds;[66] sadly, common practice in the trade shows that it does not.

Stability again In Figure 4 we saw that AuO remained unstable relative to the elements from ~2 GPa up to ~370 GPa. That was a result obtained with the PBEsol functional. When the calculations are repeated with a hybrid HSE06 functional, one obtains somewhat different results, shown in Table 1 – AuO is then unstable relative to the elements in the pressure range 80-300 GPa. The discrepancy between both methods is substantial in both low- and high-p regime, and it emphasizes shortcomings of standard DFT in dealing with strongly-correlated systems. However, the energetic stability of AuO at 1 atm in the ground state (it would be unstable with respect to O_2 formation at ambient conditions), and its re-entrant stability at pressures exceeding 300 GPa (assisted by its dynamic stability, cf. SI) jointly suggest that this compound might constitute a viable synthesis target, especially at low temperatures.

Table 1. Comparison of enthalpies concerning the Au + ½ O_2 → AuO reaction. Cubic Au was found to be more stable then the hexagonal form of gold at all pressures. Concerning oxygen, the α-form was considered at 0 GPa and the ε-form at elevated pressures.

Enthalpies per f.u. (HSE06)			
GPa	**AuO**	**Au+ ½ O_2**	**ΔH /eV**
0	**–12.444**	–12.533	**–0.089**
100	1.531	**1.415**	+0.116
200	12.480	**12.419**	+0.061
300	22.334	**22.328**	+0.006
400	**31.405**	31.503	**–0.098**
450	**35.725**	35.878	**–0.153**

4. CONCLUSIONS

AuO is an as yet unsynthesized oxide of a noble metal. With the ionic radius of Au(II) *ca.* 1.33 Å,[67] the ionic radius of oxide dianion of 1.24-1.28 Å, and using Pauling's rules, one might expect AuO to adopt the CsCl structure. However, the formal d^9 half-occupation of atomic 5d orbital of gold, close to the shell filling, is associated with partial occupation of gold-oxygen antibonding orbitals, and leads to strong vibronic effects which result in structural distortions. Moreover, the possibility of disproportionation to Au(III) (d^8) and Au(I) (d^{10}) adds to the complexity.

At p=1 atm, we predict for AuO a disproportionated structure (in that aspect like AgO but differing from CuO) with discrete square planar Au(III) and linear Au(I) ions. The calculated *C*-centered monoclinic structure is characterized by aurophilic interactions between the Au(I) ions, but is quite open. Standard DFT-GGA predicts it to be metallic, but using hybrid functionals we find it should have a small band gap of ~0.27 eV. As such, the compound should be black and possibly very reactive (in the sense of reaction kinetics). The calculated phonon spectrum of AuO shows no imaginary modes, and thus this phase should be dynamically stable – and potentially observable.

Elevation of pressure to a mere 0.8 GPa leads to a more compact AgO-type primitive monoclinic structure which is semiconducting. At p~82 GPa comproportionation occurs, in a remarkable $AuSO_4$-related structure that features Au_2O_6 units, with genuine Au(II)-Au(II) bonding and familiar square planar coordination of Au(II) cations.[62,63] All gold atoms are equivalent in this phase. At still higher pressures, above p=105 GPa, we predict transition of the oxide to the *C*-centered orthorhombic polytype, which is again disproportionated, and still semiconducting. This *C*ccm polymorph is stable up to ~329 GPa; it features classical square planar Au(III)O_4 and dumbbell Au(I)O_2 units. Notably, the geometrical preferences of gold cations at this pressure resemble those exhibited at 1 atm.

The phase transition at ~329 GPa leads to distorted NaCl-type and CsCl-type structures, with metallization occurring at the onset of stability of the orthorhombic *Cmmm* phase. Thus, metallization of AuO is predicted to occur at

much higher pressure than that of related AgO (~45 GPa).[43] AuO is again comproportionated up to 400 GPa, the highest pressure studied here.

Stability of AuO as a function of pressure and with respect to elements as well as other gold oxides is naturally of interest. This is actually a very rich topic since gold exhibits a broad range of oxidation states from –1 to +5 (even with +7 sometimes discussed[68,69]), which gives rise to a multitude of stoichiometries. including mixed-valence compounds and sub-valent phases.[70,71] Moreover, many oxidation states of gold are prone to disproportionation,[72] which results in structural complexity (just like for AuO studied here). Last but not least, correct treatment of disproportionated compounds usually necessitates the use of hybrid DFT methods, which are very time consuming. This is why the issue of thermodynamic stability of AuO in a broad pressure range will be discussed in a separate contribution, together with many other stoichiometries in the Au/O phase diagram.

ASSOCIATED CONTENT

Supporting Information

Crystallographic data of AuO structural candidates, electronic band structures and DOS, structures along B1-B2 transition paths, AuO-*C2/c* zone center phonon frequencies.

AUTHOR INFORMATION

Corresponding Authors

* Email: a.hermann@ed.ac.uk, mariana@icm.edu.pl

Notes

The authors declare no competing financial interests.

ACKNOWLEDGEMENTS

AH and RH are grateful for support from EFree, an Energy Frontier Research Center funded by the U.S. Department of Energy (Grant No. DESC0001057 at Cornell), and from the U.S. National Science Foundation (Grant

No. CHE-0910623). WG and MD acknowledge financial support from Polish National Science Centre (NCN, project HP No.2012/06/M/ST5/00344). Computational resources provided by the Cornell NanoScale Facility (supported by the National Science Foundation through Grant No. ECS-0335765), the XSEDE network (provided by the National Center for Supercomputer Applications through Grant No. TG-DMR060055N), the KAUST Supercomputing Laboratory (Project ID k128) and the UK National Supercomputing Service (ARCHER project ID d56) are gratefully acknowledged. Calculations at Univ. of Warsaw were performed on ICM machines within project G29-3.

REFERENCES

(1) Shi, H.; Asahi, R.; Stampfl, C. *Phys. Rev. B* **2007**, *75*, 205125.

(2) Grochala, W.; Mazej, Z. *Philos. Trans. R. Soc. A Math. Phys. Eng. Sci.* **2015**, *373*, 20140179–20140179.

(3) Cotton, F. A.; Wilkinson, G.; Murillo, C. A.; Bochmann, M. *Advanced Inorganic Chemistry*; 6th ed.; John Wiley & Sons Inc.: New York, 1999.

(4) Steiner, P.; Hüfner, S.; Kinsinger, V.; Sander, I.; Siegwart, B.; Schmitt, H.; Schulz, R.; Junk, S.; Schwitzgebel, G.; Gold, A.; Politis, C.; Müller, H. P.; Hoppe, R.; Kemmler-Sack, S.; Kunz, C. *Z. Phys. B* **1988**, *69*, 449–458.

(5) Burdett, J. K.; Kulkarni, G. V. *Phys. Rev. B* **1989**, *40*, 8908–8932.

(6) Gao, L.; Xue, Y. Y.; Chen, F.; Xiong, Q.; Meng, R. L.; Ramirez, D.; Chu, C. W.; Eggert, J. H.; Mao, H.-K. *Phys. Rev. B* **1994**, *50*, 4260–4263.

(7) Kresse, G.; Furthmüller, J. *Phys. Rev. B* **1996**, *54*, 11169–11186.

(8) Kresse, G. From ultrasoft pseudopotentials to the projector augmented-wave method. *Phys. Rev. B* **1999**, *59*, 1758–1775.

(9) Blöchl, P. E. *Phys. Rev. B* **1994**, *50*, 17953–17979.

(10) Perdew, J. P.; Burke, K.; Ernzerhof, M. Generalized Gradient Approximation Made Simple. *Phys. Rev. Lett.* **1996**, *77*, 3865–3868.

(11) Perdew, J.; Ruzsinszky, A.; Csonka, G. I.; Vydrov, O. A.; Scuseria, G. E.; Constantin, L. A.; Zhou, X.; Burke, K. *Phys. Rev. Lett.* **2008**, *100*, 136406.

(12) Heyd, J.; Scuseria, G. E.; Ernzerhof, M. *J. Chem. Phys.* **2006**, *124*, 219906.

(13) Lonie, D. C.; Zurek, E. *Comput. Phys. Commun.* **2011**, *182*, 372–387.

(14) Zurek, E.; Hoffmann, R.; Ashcroft, N. W.; Oganov, A. R.; Lyakhov, A. O. *Proc. Natl. Acad. Sci. U. S. A.* **2009**, *106*, 17640–3.

(15) Hermann, A.; Ashcroft, N. W.; Hoffmann, R. *Proc. Natl. Acad. Sci. U. S. A.* **2012**, *109*, 745–750.

(16) Hermann, A.; Ashcroft, N. W.; Hoffmann, R. *J. Chem. Phys.* **2014**, *141*, 024505.

(17) Hermann, A.; Schwerdtfeger, P. *J. Phys. Chem. Lett.* **2014**, *5*, 4336–4342.

(18) Hermann, A.; Ashcroft, N. W.; Hoffmann, R. *Inorg. Chem.* **2012**, *51*, 9066–75.

(19) Haas, P.; Tran, F.; Blaha, P. *Phys. Rev. B* **2009**, *79*, 085104.

(20) Csonka, G. I.; Perdew, J. P.; Ruzsinszky, A.; Philipsen, P. H. T.; Lebègue, S.; Paier, J.; Vydrov, O. A.; Ángyán, J. G. *Phys. Rev. B - Condens. Matter Mater. Phys.* **2009**, *79*, 1–14.

(21) Scherbaum, F.; Grohmann, A.; Huber, B.; Krüger, C.; Schmidbaur, H. *Angew. Chemie Int. Ed.* **1988**, *27*, 1544–1546.

(22) Schmidbaur, H. *Gold Bull.* **2000**, *33*, 3–10.

(23) Pyykkö, P. *Chem. Rev.* **1997**, *97*, 597–636.

(24) Niggli, P. *Z. Kristallogr.* **1922**, *57*, 253–299.

(25) Tunell, G.; Posnjak, E.; Ksanda, C. J. *Z. Kristallogr.* **1935**, *90*, 120–142.

(26) Derzsi, M.; Hermann, A.; Hoffmann, R.; Grochala, W. *Eur. J. Inorg. Chem.* **2013**, 5094–5102.

(27) Keinan, S.; Avnir, D. *Inorg. Chem.* **2001**, *40*, 318–23.

(28) Smith, D. W. *Coord. Chem. Rev.* **1976**, *21*, 93–158.

(29) Levi, G. R.; Fontana, C. *Gazz. Chim. Ital.* **1926**, *56*, 388–396.

(30) Moore, W. J.; Pauling, L. *J. Am. Chem. Soc.* **1941**, *63*, 1392–1394.

(31) McMillan, J. A. *J. Inorg. Nucl. Chem.* **1960**, *13*, 28–31.

(32) Brese, N. E.; O'Keeffe, M.; Ramakrishna, B. L.; Von Dreele, R. B. *J. Solid State Chem.* **1990**, *89*, 184–190.

(33) Derzsi, M.; Piekarz, P.; Grochala, W. *Phys. Rev. Lett.* **2014**, *113*, 025505.

(34) Lawton, S. L.; Rohrbaugh, W. J.; Kokotailo, G. T. *Inorg. Chem.* **1972**, *11*, 2227–2233.

(35) Dedieu, A.; Hoffmann, R. *J. Am. Chem. Soc.* **1978**, *100*, 2074–2079.

(36) Thorn, D. L.; Hoffmann, R. *J. Am. Chem. Soc.* **1978**, *100*, 2079–2090.

(37) Jiang, Y.; Alvarez, S.; Hoffmann, R. *Inorg. Chem.* **1985**, *24*, 749–757.

(38) Burdett, J. K.; Eisenstein, O.; Schweizer, W. B. *Inorg. Chem.* **1994**, *33*, 3261–3268.

(39) Pyykkö, P.; Zhao, Y. *Angew. Chemie Int. Ed.* **1991**, *30*, 604–605.

(40) Pyykkö, P. *Angew. Chemie Int. Ed.* **2004**, *43*, 4412–56.

(41) Doll, K.; Pyykkö, P.; Stoll, H. *J. Chem. Phys.* **1998**, *109*, 2339.

(42) Allen, J. P.; Scanlon, D. O.; Watson, G. W. *Phys. Rev. B Rapid Comm.* **2010**, *81*, 161103.

(43) Włodarska, I.; Derzsi, M.; Grochala, W. *Phys. status solidi - Rapid Res. Lett.* **2015**, *9*, 401–404.

(44) Barrett, C. S.; Meyer, L.; Wasserman, J. *J. Chem. Phys.* **1967**, *47*, 592–597.

(45) Neaton, J. B.; Ashcroft, N. W. *Phys. Rev. Lett.* **2002**, *88*, 205503.

(46) Wickleder, M. S. *Zeitschrift fuer Anorg. und Allg. Chemie* **2001**, *627*, 2112.

(47) Westrik, R. *Acta Crystallogr.* **1954**, *7*, 764–767.

(48) Pascard, R.; Pascard-Billy, C. *Acta Crystallogr.* **1965**, *18*, 830–834.

(49) Bader, R. F. W. *Atoms in Molecules: A Quantum Theory*; Oxford University Press: Oxford, UK, 1994.

(50) Jarchow, O.; Schulz, H.; Nast, R. *Angew. Chemie Int. Ed.* **1970**, *9*, 71–71.

(51) Goggin, P. L.; Goodfellow, R. J. *Dalt. Trans.* **1973**, 2355.

(52) Doonan, D. J.; Balch, A. L.; Goldberg, S. Z.; Eisenberg, R.; Miller, J. S. *J. Am. Chem. Soc.* **1975**, *97*, 1961–1962.

(53) Xu, Q.; Heaton, B. T.; Jacob, C.; Mogi, K.; Ichihashi, Y.; Souma, Y.; Kanamori, K.; Eguchi, T. *J. Am. Chem. Soc.* **2000**, *122*, 6862–6870.

(54) Holloway, R. G.; Penfold, B. R.; Colton, R.; McCormick, M. J. *Chem. Commun.* **1976**, 485.

(55) Brown, M. P.; Puddephatt, R. J.; Rashidi, M.; Manojlović-Muir, L.; Muir, K. W.; Solomun, T.; Seddon, K. R. *Inorg. Chim. Acta* **1977**, *23*, L33–L34.

(56) Miedaner, A.; DuBois, D. L. *Inorg. Chem.* **1988**, *27*, 2479–2484.

(57) Hoffman, D. M.; Hoffmann, R. *Inorg. Chem.* **1981**, *20*, 3543–3555.

(58) Vegas, A.; Jansen, M. *Acta Crystallogr. Sect. B Struct. Sci.* **2002**, *58*, 38–51.

(59) Buerger, M. J. In *Phase Transformations in Solids*; Smoluchowski, R.; Mayer, J. E.; Weyl, W. A., Eds.; John Wiley & Sons Inc.: New York, 1951; pp. 183–211.

(60) Watanabe, M.; Tokonami, M.; Morimoto, N. *Acta Cryst. A* **1977**, *33*, 294–298.

(61) Tolédano, P.; Knorr, K.; Ehm, L.; Depmeier, W. *Phys. Rev. B* **2003**, *67*, 144106.

(62) Einstein, F. W. B.; Rao, P. R.; Trotter, J.; Bartlett, N. *J. Chem. Soc. A Inorganic, Phys. Theor.* **1967**, 478.

(63) Seidel, S.; Seppelt, K. *Science (80-.).* **2000**, *290*, 117–118.

(64) Pearson, R. G. *Acc. Chem. Res.* **1993**, *26*, 250–255.

(65) Shimizu, K.; Suhara, K.; Ikumo, M.; Eremets, M. I.; Amaya, K. *Nature* **1998**, *393*, 767.

(66) Zurek, E.; Grochala, W. *Phys. Chem. Chem. Phys.* **2015**, *17*, 2917–2934.

(67)

(68) Riedel, S.; Kaupp, M. *Inorg. Chem.* **2006**, *45*, 1228–1234.

(69) Pyykkö, P. *Chem. Soc. Rev.* **2008**, *37*, 1967–97.

(70) Lee, H. M.; Lee, K. H.; Lee, G.; Kim, K. S. *J. Phys. Chem. C* **2015**, 150615095155002.

(71) Citra, A.; Andrews, L. *J. Mol. Struct. THEOCHEM* **1999**, *489*, 95–108.

(72) Kurzydłowski, D.; Grochala, W. *Chem. Commun.* **2008**, *1*, 1073.

Table of Contents Synopsis

We study from first-principles the structural and electronic properties of hypothetical gold(II) oxide, AuO, at ambient and elevated pressures. We find that AuO is a small gap semiconductor at atmospheric pressure, crystallizes in a new structure type as disproportionated Au(I)Au(III)O_2, and is stabilized by aurophilic interactions. By applying pressure, a sequence of com- and disproportionated AuO structures becomes stable, but metallization is delayed up to about 3 million atmospheres.

Table of Contents Graphics